

# The Effect of Electrospinning Precursor Flow Rate with Rotating Collector on ZnO Nanofiber Size Results on Double-Layered DSSC Photoanode Fabrication

Widhiyanuriyawan, Denny

Department of Mechanical Engineering, Universitas Brawijaya

Arifin, Zainal

Department of Mechanical Engineering, Universitas Sebelas Maret

Muwaffaq, Abyan

Department of Mechanical Engineering, Universitas Sebelas Maret

Suyitno, Suyitno

Department of Mechanical Engineering, Universitas Sebelas Maret

他

<https://doi.org/10.5109/6782154>

---

出版情報 : Evergreen. 10 (1), pp.504-509, 2023-03. 九州大学グリーンテクノロジー研究教育センターバージョン :

権利関係 : Creative Commons Attribution-NonCommercial 4.0 International

# The Effect of Electrospinning Precursor Flow Rate with Rotating Collector on ZnO Nanofiber Size Results on Double-Layered DSSC Photoanode Fabrication

Denny Widhiyanuriyawan<sup>1,\*</sup>, Zainal Arifin<sup>2</sup>, Abyan Muwaffaq<sup>2</sup>, Suyitno Suyitno<sup>2</sup>, Syamsul Hadi<sup>2</sup>, Singgih Dwi Prasetyo<sup>2</sup>, and Bayu Sutanto<sup>3</sup>

<sup>1</sup>Department of Mechanical Engineering, Universitas Brawijaya, Malang 65145, Indonesia

<sup>2</sup>Department of Mechanical Engineering, Universitas Sebelas Maret, Surakarta 57126, Indonesia

<sup>3</sup>Department of Mechanical Engineering, The University of Manchester, Manchester, United Kingdom

\*Author to whom correspondence should be addressed:

E-mail: denny\_w@ub.ac.id

(Received September 6, 2022; Revised March 24, 2023; accepted March 24, 2023).

**Abstract:** DSSC solar cells are predicted to be energy conversion devices for the next generation; therefore, various developments are carried out to improve the performance of DSSC solar cells. In this paper, we present the results of research on the process of using ZnO nanofibers as DSSC photoanodes using an electrospinning machine. The direct deposition method was used to directly spray the ZnO precursor solution on conductive glass deposited with TiO<sub>2</sub>. The rotating collector was used to make uniform and reduce the size of the resulting nanofiber structure. The size reduction in the resulting nanofiber can improve the performance of DSSC photoanode. Variations of a precursor discharge of 2, 4, 6, and 8  $\mu\text{L}/\text{minute}$  were used to determine the effects on the morphological arrangement of the resulting ZnO nanofibers. From the results of this study, the most uniform nanofiber results and the smallest average size were obtained from the use of the lowest flow rate variation, which was 2 ml/minute.

Keywords: DSSC; electrospinning; rotating collector; variations of precursor discharge

## 1. Introduction

The increasing need for energy use by humans demands scientists to research and develop the use of renewable energy sources as an alternative<sup>1-3</sup>). One of the renewable energy options is solar energy due to its abundant availability and sustainable energy supply<sup>4</sup>). A solar cell is a device that converts solar energy into electrical energy<sup>5</sup>). The latest generation of three generations of solar cells developed by scientists is the dye-sensitized solar cell (DSSC), which was discovered by Michael Gratzel in 1991<sup>6</sup>).

DSSC has several advantages such as low fabrication costs, flexibility, and more environmentally friendly materials<sup>6</sup>). The DSSC component consists of a TCO substrate, semiconductor, dye, electrolyte, and counter electrode<sup>7,8</sup>). The working principle of DSSC utilizes photon energy to excite electrons from the dye to generate electricity from the oxidation–reduction cycle that occurs in the DSSC<sup>9</sup>). DSSC performance is indicated by efficiency ( $\eta$ ), short-circuit current density ( $J_{sc}$ ), fill factor (FF), and open-circuit voltage ( $V_{oc}$ )<sup>10</sup>).

The value of DSSC performance depends on the type of

semiconductor fabrication used in its preparation<sup>11,12</sup>). In general, TiO<sub>2</sub> and ZnO are used as DSSC semiconductors. TiO<sub>2</sub> has the advantage of low cost and good performance in ultraviolet light, although its performance is quite poor in visible and infrared light<sup>13</sup>). ZnO has the advantage of higher electron mobility and is easy to modify on its morphological structure, although ZnO has a low level of chemical stability and a higher band gap than TiO<sub>2</sub><sup>14-16</sup>). The double-layer method is used to form a dye loading layer using TiO<sub>2</sub> and a light scattering layer using ZnO, with the purpose of strengthening the bonds between semiconductor and substrate, expanding the light absorption range by using dye as a sensitizer, expanding the area of dye absorption, and increasing capture of photons<sup>17,18</sup>). Figure 1 shows a DSSC with double-layered photoanode.

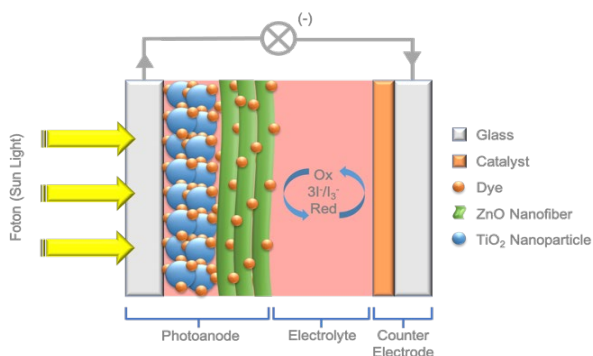


Figure 1. DSSC structure.

A nanofiber is one type of nanostructure used for a DSSC photoanode. A nanofiber has a morphological structure that can provide a direct flow of electrons from the photogenerated current to its conductive substrate and has a dendrite-like structure that results in a larger absorption surface area<sup>19</sup>. The electrospinning process is one way to produce nanofibers. Some of the advantages of electrospinning include a low-cost fabrication process and ability to control the morphology of the resulting fiber<sup>20</sup>. The working principle of electrospinning is to use electrostatic forces formed from charged particles caused by the emergence of high voltage between the needle tip and the collector<sup>21–24</sup>. Figure 2 shows a picture of electrospinning and its components.

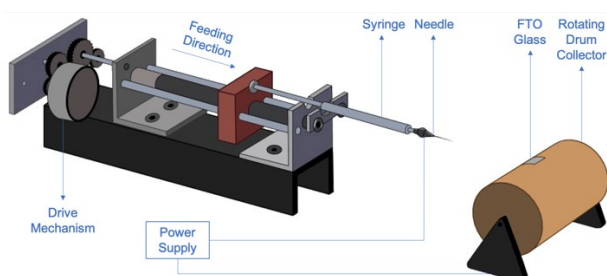


Fig. 2: Electrospinning machine with rotating collector.

The morphological structure of the electro spun nanofibers is influenced by several factors, one of which is the precursor flow rate during the feeding process. The higher the flow rate used, the thicker the nanofibers formed<sup>20</sup>. The use of a rotating collector in the electrospinning process will also provide better uniformity of the resulting nanofibers, as well as increase the rate of precursor evaporation, which will affect the decrease in nanofiber diameter<sup>25</sup>. The smaller the size of the resulting nanofiber, the higher the increase in performance of the DSSC<sup>26</sup>. Previous studies varied the precursor flow rate in the electrospinning process with a fixed collector, resulting in the smallest average nanofiber diameter at the lowest flow rate, although the use of a fixed collector resulted in poor uniformity and defects in the resulting nanofibers<sup>27</sup>.

The aim of this research to determine the effect of electrospinning flow rate on rotating collectors. The

precursor solution was made using a mixture of polyvinyl alcohol solution with zinc acetate solution. The direct deposition method was used to place the semiconductor to the substrate. This method was performed by spraying the precursor solution directly onto the TiO<sub>2</sub>-deposited conductive glass in the electrospinning process. The use of this method shortened the ZnO coating process in the manufacture of DSSC and reduced damage to the nanofiber results<sup>28–31</sup>. Variation in the precursor flow rate was used to determine its effect on the resulting nanofiber.

## 2. Methods

### 2.1 Semiconductor Fabrication and Sintering Process

The process began by synthesizing a precursor solution consisting of a mixture of polyvinyl alcohol (PVA, made by Merck) solution and a zinc acetate solution. The PVA solution was prepared by dissolving 1 gram of polyvinyl alcohol ((C<sub>2</sub>H<sub>4</sub>O)<sub>x</sub>) with 10 ml of distilled water, then stirring for the homogenization process for 4 × 60 minutes at a temperature of 158°F. The Zn (CH<sub>3</sub>CO<sub>2</sub>)<sub>2</sub> solution was synthesized by dissolving 2 grams of zinc acetate dihydrate ((CH<sub>3</sub>COO)<sub>2</sub>Zn.2H<sub>2</sub>O, made by Merck) in 8 ml of distilled water, then stirring for the homogenization process for 60 minutes at 158°F. Next, the PVA solution was mixed with the Zn (CH<sub>3</sub>CO<sub>2</sub>)<sub>2</sub> solution in a ratio of 4:1 wt%, then stirred for the homogenization process for 8 × 60 minutes at a temperature of 158°F. Then, the mixed solution was left at room temperature for 24 hours to remove the resulting foam. The result was a solution of PVA/Zn (CH<sub>3</sub>CO<sub>2</sub>)<sub>2</sub>, which can be used to compose ZnO nanofibers using an electrospinning machine.

The PVA/Zn (CH<sub>3</sub>CO<sub>2</sub>)<sub>2</sub> solution was then put into a syringe pump with a capacity of 1 ml and installed in electrospinning machine. The syringe containing the solution was connected to the positive pole of a 15 kV high voltage and placed at a fixed distance of 8 cm from the FTO (fluorine doped tin oxide) glass on the rotating collector connected to the negative pole. An FTO glass that had been deposited with TiO<sub>2</sub> nanoparticles was used in this study. The precursor flow rate as an independent variable in the electrospinning process used variations of 2, 4, 6, and 8 μL/minute. The solution that was sprayed from the syringe was subjected to high voltage, so that the electrostatic field on the negatively charged collector would attract the solution to the FTO glass. The solution then automatically adhered to the collector surface in the form of nanofibers. After the spraying process, the samples were sintered at a temperature of about 932°F for 60 minutes to dissolve the organic matter and form ZnO into crystals.

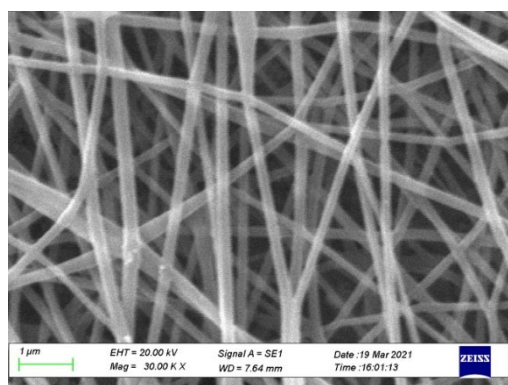
## 3. Results and Discussion

### 3.1 DSSC Characteristic Test

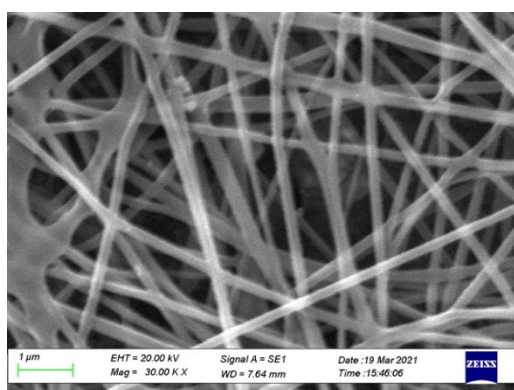
The Scanning Electron Microscope (SEM) test

produces graphic data in the form of structure and dimensions of ZnO semiconductor nanofibers. The results of the SEM test of the double-layer DSSC photoanode are shown in Figure 3. From the photo of the SEM test results, it can be observed that the lower the use of the precursor flow rate, the smaller the diameter of the resulting nanofiber. The SEM test results from the DSSC photoanode with the electrospinning process using a rotating collector drum were much more uniform than using a fixed collector, as in previous studies<sup>27)</sup>. This proves previous research, which explains that the use of a rotating collector will produce nanofibers with good uniformity<sup>25)</sup>.

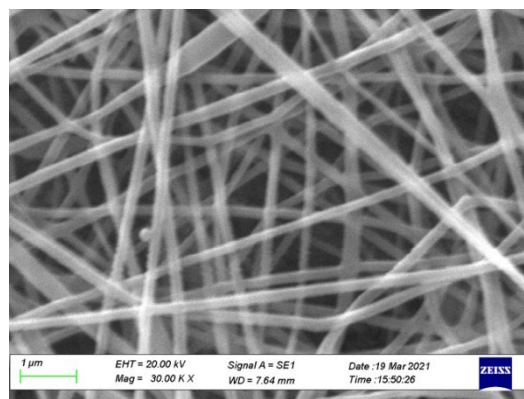
In Fig. 3, the SEM test results are shown with various variations of precursor flow rates. Fig. (3.a) is the smallest diameter of nanofibers that can be produced by precursor flow rate 2  $\mu\text{L}/\text{minute}$ , while Fig (3.d) shows the size of the largest nanofiber diameter which produced by precursor flow rate 8  $\mu\text{L}/\text{minute}$ . So that a low precursor flow rate can result in a smaller nanofiber diameter as well. The smaller size of the nanofiber fibers can facilitate the electron transfer process that occurs in DSSC cells, so that the overall working efficiency of the cell can be improved.



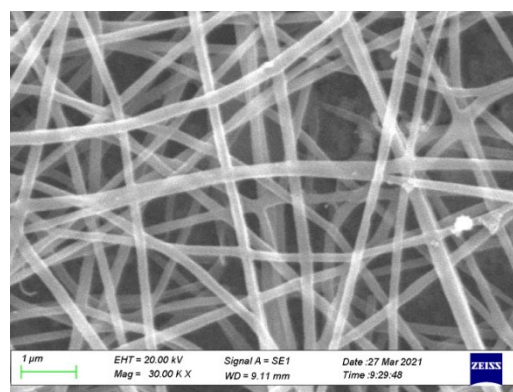
(a)



(b)



(c)



(d)

**Fig. 3:** Double-layer photoanode SEM test results for precursor flow rate variation. (a) 2  $\mu\text{L}/\text{minute}$ , (b) 4  $\mu\text{L}/\text{minute}$ , (c) 6  $\mu\text{L}/\text{minute}$ , and (d) 8  $\mu\text{L}/\text{minute}$ .

However, some defects were still found in the nanofiber results. This is because the stretching process of the solution that comes out of the syringe tip is influenced by whether the voltage used in the electrospinning process is constant. The stretching process of the solution will also take more time as the flow rate of the precursor used increases, which in turn causes some of the solution to not adhere perfectly to the substrate. This proves previous research, which explains that the uniformity of the resulting nanofiber will be better with the use of a lower flow rate of precursor<sup>32)</sup>, while the possibility of defects in the resulting nanofiber will be greater along with the magnitude of the flow rate of the precursor used<sup>33)</sup>.

The results of the nanofiber diameter measurements using ImageJ software can be seen in Table 1.

Table 1. Measurement of the diameter of ZnO nanofibers for each variation of precursor flow rate.

Precursor flow rate variation	Average diameter (nm)	Maximum diameter (nm)	Minimum diameter (nm)
2 $\mu\text{L}/\text{minute}$	127.078	139.022	114.683
4 $\mu\text{L}/\text{minute}$	186.266	194.906	179.428
6 $\mu\text{L}/\text{minute}$	224.657	239.798	207.959



8 $\mu\text{L}/\text{minute}$	287.052	298.299	271.92
-------------------------------	---------	---------	--------

8 $\mu\text{L}/\text{minute}$	0.59	6.01	45.17	1.59
-------------------------------	------	------	-------	------

These data show that the use of a larger precursor flow rate produced nanofibers with a larger diameter. The results of this measurement are in accordance with previous studies, which explained that the thickness of the nanofiber produced from the electrospinning process is directly proportional to the flow rate of the precursor used<sup>20</sup>. The use of a rotating collector also increased the evaporation rate of the precursor to produce nanofibers with a smaller diameter compared to the use of a fixed collector in previous studies<sup>27</sup>. This supports a previous study, which explained that the use of a rotating collector will cause the nanofiber diameter to be relatively smaller<sup>25</sup>. The size reduction in the nanofiber produced either from the use of low flow rate variations or the use of a rotating drum collector will increase the dye absorption area by the semiconductor, which will increase the performance of the DSSC<sup>26</sup>.

### 3.2 DSSC performance Test

DSSC performance test was performed using a solar simulator at an ultraviolet intensity of 100 mW/cm<sup>2</sup>. From this test, the current-voltage curve for each variation of the precursor flow rate in the manufacturing process of double-layer DSSC photoanode can be obtained as shown in Figure 5. From this test, the characteristic data of DSSC for each variation can also be seen in Table 2.

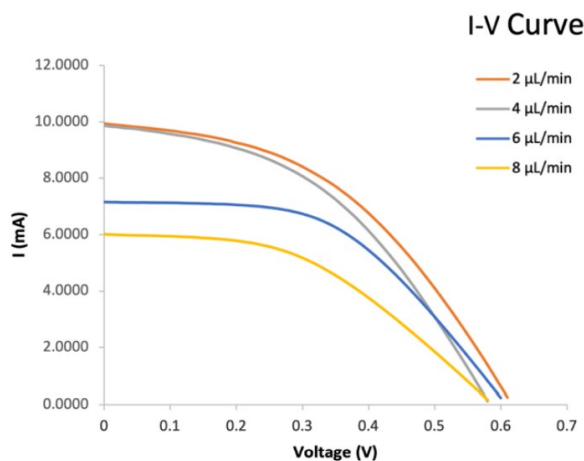


Fig.4 I-V curve of DSSC for each variation

Table 2. Characteristic data of DSSC for each variation

Precursor flow rate variation	V <sub>oc</sub> (V)	J <sub>sc</sub> (Ma/cm <sup>2</sup> )	FF (%)	$\eta$ (%)
2 $\mu\text{L}/\text{minute}$	0.61	9.93	44.47	2.72
4 $\mu\text{L}/\text{minute}$	0.58	9.87	41.58	2.53
6 $\mu\text{L}/\text{minute}$	0.60	7.15	50.82	2.21

From the test results shown previously, it can be observed that the DSSC made with small amount of precursor flow rate variation is more efficient than the higher one. The variation of precursor flow rate 2  $\mu\text{L}/\text{min}$  resulted in the value of V<sub>OC</sub> by 0.61 V, the value of J<sub>SC</sub> by 9.93 mA/cm<sup>2</sup>, the fill factor percentage by 44.47%, and the efficiency percentage by 2.72%. The variation of precursor flow rate 4  $\mu\text{L}/\text{min}$  resulted in the value of V<sub>OC</sub> by 0.58 V, the value of J<sub>SC</sub> by 9.87 mA/cm<sup>2</sup>, the fill factor percentage by 41.58%, and the efficiency percentage by 2.53%. The variation of precursor flow rate 6  $\mu\text{L}/\text{min}$  resulted in the value of V<sub>OC</sub> by 0.60 V, the value of J<sub>SC</sub> by 7.15 mA/cm<sup>2</sup>, the fill factor percentage by 50.82%, and the efficiency percentage by 2.21%. The variation of precursor flow rate 8  $\mu\text{L}/\text{min}$  resulted in the value of V<sub>OC</sub> by 0.59 V, the value of J<sub>SC</sub> by 6.01 mA/cm<sup>2</sup>, the fill factor percentage by 45.17%, and the efficiency percentage by 1.59%.

The increasing trend of the J<sub>SC</sub> value along with the smaller variations in the flow rate used indicates that more electric current is converted from solar energy, thereby increasing the percentage value of efficiency. The increase in DSSC performance is obtained when the precursor flow rate used in electrospinning process is in small amount, the smaller the amount of precursor flow rate, the more time available for the precursor evaporation process to actually stick to the collector. This is in accordance with previous studies which explained that the lower the flow rate of the precursor used, the more time sufficient for the precursor to evaporate and adhere perfectly to the collector, resulting in nanofibers with smaller diameters and better uniformity. The use of a rotating drum collector also increases the evaporation rate of the precursor so as to produce nanofibers with a smaller diameter compared to the use of a collector fixed as in previous studies<sup>27</sup>. This is in accordance with previous research which explained that the use of a rotating drum collector affects the diameter of the nanofiber to be relatively smaller. The smaller the size of the nanofiber produced, either from the use of low flow rate variations or the use of a rotating drum collector, will increase the dye absorption area by the semiconductor which has an impact on increasing the performance of the DSSC<sup>34</sup>.

### 4. Conclusion

In this study, we have succeeded in studying the effect of electrospinning Precursor Flow Rate with Rotating Collector have been done. The use of variations in the precursor flow rate in electrospinning process with a rotating drum collector using direct deposition method affects the characteristics and performance of the resulting double-layer DSSC photoanode. The use of rotating drum collector also affects the size of the resulting nanofiber to be relatively smaller than the use of a fixed collector. The

lower the flow rate of the precursor used, the smaller the resulting nanofiber diameter and the wider the dye absorption area, so that the DSSC performance will increase. The highest efficiency was obtained by DSSC with a variation of the precursor flow rate of 2  $\mu\text{L}/\text{min}$ , with the efficiency percentage of 2.72%, followed by the value VOC by 0.61 V, the value of JSC by 9.93  $\text{mA}/\text{cm}^2$ , and fill factor percentage by 44.47%.

### Acknowledgements

This work was partially supported by the grant of PDUPT from the Ministry of Research, Technology, and Higher Education, the Republic of Indonesia with contract number 719/UN.27.21/PN/2019 for FY 2019.

### Nomenclature

<i>DSSC</i>	dye-sensitized solar cell
$E_{\text{band gap}}$	band gap energy (eV)
$E_{\text{HOMO}}$	HOMO energy (eV)
$E_{\text{LUMO}}$	LUMO energy (eV)
$E_{\text{ox}}$	oxidation energy (eV)
$E_{\text{red}}$	reduction energy (eV)
<i>FF</i>	fill factor
<i>FTO</i>	fluorine-doped tin oxide
<i>HOMO</i>	highest occupied molecular orbital
<i>HPA</i>	heteropolyacid
<i>I-V</i>	current-voltage
$I_{\text{SC}}$	short circuit current (A)
<i>LUMO</i>	lowest unoccupied molecular orbital
$P_{\text{MPP}}$	maximum power point (W)
$V_{\text{OC}}$	open circuit voltage (V)

### Greek symbols

$\eta$	efficiency (%)
--------	----------------

### Subscripts

<i>ox</i>	oxidation
<i>rad</i>	radiation
<i>red</i>	reduction

### References

- 1) N. Kannan, and D. Vakeesan, "Solar energy for future world: - a review," **62** 1092–1105 (2016). doi:10.1016/j.rser.2016.05.022.
- 2) T. Hanada, "Modifying the feed-in tariff system in japan : an environmental perspective," *Evergreen*, **3** (2) 54–58 (2016). doi:10.5109/1800872.
- 3) M. Khanam, M.F. Hasan, T. Miyazaki, B. Baran, and S. Koyama, "Key factors of solar energy progress in bangladesh until 2017," *Evergreen*, **5** (2) 78–85 (2018). doi:10.5109/1936220.
- 4) M. Shakeel, A.K. Pandey, and N. Abd, "Advancements in the development of tio 2 photoanodes and its fabrication methods for dye sensitized solar cell ( dssc ) applications . a review," *Renew. Sustain. Energy Rev.*, **77** (April) 89–108 (2017). doi:10.1016/j.rser.2017.03.129.
- 5) Z. Arifin, S. Suyitno, S. Hadi, and B. Sutanto, "Improved performance of dye-sensitized solar cells with tio2 nanoparticles/zn-doped tio2 hollow fiber photoanodes," *Energies*, **11** (11) (2018). doi:10.3390/en11112922.
- 6) B. Boro, B. Gogoi, B.M. Rajbongshi, and A. Ramchiary, "Nano-structured tio2/zno nanocomposite for dye-sensitized solar cells application: a review," *Renew. Sustain. Energy Rev.*, **81** (May 2017) 2264–2270 (2018). doi:10.1016/j.rser.2017.06.035.
- 7) M. Grätzel, "Solar energy conversion by dye-sensitized photovoltaic cells," *Inorg. Chem.*, **44** (20) 6841–6851 (2005). doi:10.1021/ic0508371.
- 8) Z. Arifin, S. Hadi, Suyitno, B. Sutanto, and D. Widhiyanuriyawan, "Investigation of curcumin and chlorophyll as mixed natural dyes to improve the performance of dye-sensitized solar cells," *Evergreen*, **9** (1) 17–22 (2022). doi:10.5109/4774212.
- 9) M.S.W. Kumara, and G. Prajitno, "Studi awal fabrikasi dye sensitized solar cell (dssc) dengan menggunakan ekstraksi daun bayam (amaranthus hybridus l.) sebagai dye sensitizer dengan variasi jarak sumber cahaya pada dssc," (2012).
- 10) Y. Ooyama, and Y. Harima, "Photophysical and electrochemical properties, and molecular structures of organic dyes for dye-sensitized solar cells," *ChemPhysChem*, **13** (18) 4032–4080 (2012). doi:10.1002/cphc.201200218.
- 11) K.K. Tehare, S.T. Navale, F.J. Stadler, Z. He, H. Yang, X. Xiong, X. Liu, and R.S. Mane, "Enhanced dsscs performance of tio2 nanostructure by surface passivation layers," *Mater. Res. Bull.*, **99** 491–495 (2018). doi:https://doi.org/10.1016/j.materresbull.2017.11.046.
- 12) S. Sakiyama, T. Komura, H. Iwashita, N. Mizutani, and K. Fujita, "Carrier density and mobility in n-doped poly(p-phenylene vinylene)," *Evergreen*, **3** 18–20 (2016). doi:10.5109/1657382.
- 13) A. Azani, D.S. Che Halin, M.M.A.B. Abdullah, K. Abdul Razak, M. Razak, M. Ramli, M.A.A. Mohd Salleh, and V. Chobpattana, "The effect of go/tio\_2 thin film during photodegradation of methylene blue dye," *Evergreen*, **8** 556–564 (2021). doi:10.5109/4491643.
- 14) T.P. Chou, Q. Zhang, G.E. Fryxell, and G. Cao, "Hierarchically structured zno film for dye-sensitized solar cells with enhanced energy conversion efficiency," *Adv. Mater.*, **19** (18) 2588–2592 (2007). doi:10.1002/adma.200602927.
- 15) E.R. Dyartanti, I.N. Widiassa, A. Purwanto, and H.

- Susanto, "Nanocomposite polymer electrolytes in pvdf/zno membranes modified with pvp for use in lifepo4 batteries," *Evergreen*, **5** (2) 19–25 (2018). doi:10.5109/1936213.
- 16) N.B. Prihantini, N. Rakhmayanti, S. Handayani, W. Samsuridzal, W. Wardhana, and Nasruddin, "Biomass production of indonesian indigenous leptolyngbya strain on npk fertilizer medium and its potential as a source of biofuel," *Evergreen*, **7** (4) 593–601 (2020). doi:10.5109/4150512.
  - 17) S. Ito, T.N. Murakami, P. Comte, P. Liska, C. Grätzel, M.K. Nazeeruddin, and M. Grätzel, "Fabrication of thin film dye sensitized solar cells with solar to electric power conversion efficiency over 10%," *Thin Solid Films*, **516** (14) 4613–4619 (2008). doi:10.1016/j.tsf.2007.05.090.
  - 18) Z. Arifin, S. Hadi, S. Suyitno, A.R. Prabowo, and S.D. Prasetyo, "Characterization of zno nanofiber on double-layer dye-sensitized solar cells using direct deposition method," *Period. Tche Quim.*, **17** (36) 263–277 (2020). <http://www.deboni.he.com.br/Periodico36.pdf>.
  - 19) O. Lupan, V.M. Guérin, L. Ghimpu, I.M. Tiginyanu, and T. Pauporté, "Nanofibrous-like zno layers deposited by magnetron sputtering and their integration in dye-sensitized solar cells," *Chem. Phys. Lett.*, **550** 125–129 (2012). doi:10.1016/j.cplett.2012.08.071.
  - 20) B.D. Li, and Y. Xia, "Electrospinning of nanofibers : reinventing the wheel ?\*\*," (14) 1151–1170 (2004). doi:10.1002/adma.200400719.
  - 21) M.K. Nazeeruddin, E. Baranoff, and M. Grätzel, "Dye-sensitized solar cells: a brief overview," *Sol. Energy*, **85** (6) 1172–1178 (2011). doi:10.1016/j.solener.2011.01.018.
  - 22) M. Grätzel, "Perspectives for dye-sensitized nanocrystalline solar cells," *Prog. Photovoltaics Res. Appl.*, **8** 171–185 (2000). doi:10.1002/(SICI)1099-159X(200001/02)8:1%3C171::AID-PIP300%3E3.0.CO;2-U.
  - 23) M. Grätzel, "Photoelectrochemical cells," *Nature*, **414** (2001). doi:10.1038/35104607.
  - 24) C. Cornaro, L. Renzi, M. Pierro, A. Di Carlo, and A. Guglielmotti, "Thermal and electrical characterization of a semi-transparent dye-sensitized photovoltaic module under real operating conditions," *Energies*, **11** (1) (2018). doi:10.3390/en11010155.
  - 25) S. Ojha, "Structure-property relationship of electrospun fibers," Elsevier Ltd., 2017. doi:10.1016/B978-0-08-100907-9.00010-6.
  - 26) L. Yang, and W.W.-F. Leung, "Optimizing scattering layer for efficient dye sensitized solar cells based on tio2 nanofiber," *Polyhedron*, **82** 7–11 (2014). doi:<https://doi.org/10.1016/j.poly.2014.03.029>.
  - 27) M.Z. Khusaini, H.N. Jati, Suyitno, S. Hadi, and Z. Arifin, "The influence of electrospinning flow rate parameter on zno nanofiber as photoanode of dye-sensitized solar cell," *AIP Conf. Proc.*, **2217** (April) (2020). doi:10.1063/5.0000702.
  - 28) S. Suyitno, T.J. Saputra, A. Supriyanto, and Z. Arifin, "Stability and efficiency of dye-sensitized solar cells based on papaya-leaf dye," *Spectrochim. Acta - Part A Mol. Biomol. Spectrosc.*, **148** 99–104 (2015). doi:10.1016/j.saa.2015.03.107.
  - 29) Z. Arifin, S. Soeparman, D. Widhiyanuriyawan, and S. Suyitno, "Performance enhancement of dye-sensitized solar cells using a natural sensitizer," *Int. J. Photoenergy*, **2017** (2017). doi:10.1155/2017/2704864.
  - 30) W.A. Ayalew, and D.W. Ayele, "Dye-sensitized solar cells using natural dye as light-harvesting materials extracted from acanthus sennii chiovenda flower and euphorbia cotinifolia leaf," *J. Sci. Adv. Mater. Devices*, **1** (4) 488–494 (2016). doi:10.1016/j.jsamd.2016.10.003.
  - 31) B. Cerda, R. Sivakumar, and M. Paulraj, "Natural dyes as sensitizers to increase the efficiency in sensitized solar cells," *J. Phys. Conf. Ser.*, **720** (1) 1–5 (2016). doi:10.1088/1742-6596/720/1/012030.
  - 32) S. Zargham, S. Bazgir, A. Tavakoli, A.S. Rashidi, and R. Damerchely, "The effect of flow rate on morphology and deposition area of electrospun nylon 6 nanofiber," **7** (4) 42–49 (2012).
  - 33) M. Chowdhury, and G. Stylios, "Effect of experimental parameters on the morphology of electrospun nylon 6 fibres," (06) (2010).
  - 34) L. Yang, and W.W.-F. Leung, "Optimizing scattering layer for efficient dye sensitized solar cells based on tio2 nanofiber," *Polyhedron*, **82** 7–11 (2014). doi:<https://doi.org/10.1016/j.poly.2014.03.029>.